

# State-Space Averaged Model of Three-Phase Four-Wire Shunt Active Power Filter based on Current-Controlled VSI

P. Rodríguez<sup>1</sup>, J. I. Candela<sup>1</sup> and R. Pindado<sup>2</sup>

<sup>1</sup> Department of Electrical Engineering

<sup>2</sup> Department of Electronic Engineering

Universitat Politècnica de Catalunya

Colom, 1, 08222 Barcelona (Spain)

phone:+34 93 7398036, fax:+34 93 7398225,

e-mail: [prodriguez@ee.upc.es](mailto:prodriguez@ee.upc.es), [candela@ee.upc.es](mailto:candela@ee.upc.es), [pindado@eel.upc.es](mailto:pindado@eel.upc.es)

**Abstract.** This work presents a universal state-space average model of three-phase four-wire shunt active power filter based on current-controlled voltage-source inverters. In this type of inverters two topologies are commonly used, namely the Four-Leg Full-Bridge (FLFB) topology, and the Three-Leg Split-Capacitor (TLSC) topology. Combining these topologies, a third topology can be obtained, namely the Four-Leg Split-Capacitor (FLSC) topology. This last topology exhibits very interesting characteristics for active filter applications. By means study of FLSC topology a state-space average model can be obtained, which will allow long-time simulations with a low cost of computation time. The behaviour of FLFB and TLSC converters can be obtained as particular cases of this universal model. Likewise, a generic technique for injected current control is proposed, offering as main advantage a decoupled control of the different legs, so full-bridge converters can be implemented without using space-vector based current control techniques.

## Key words

Power Filters, Harmonics, Power Conditioning, Power Quality, Power Electronics.

## 1. Introduction

In recent years, three-phase four-wire shunt active power filters have appeared as an effective method to solve the problem caused by harmonic and unbalanced currents as well as to compensate load reactive power. In these filters, two topologies for current-controlled voltage source inverter are commonly used, namely the Four-Leg Full-Bridge (FLFB) topology, and the Three-Leg Split-Capacitor (TLSC) topology. These topologies, shown in Fig. 1, were presented at the beginning of the 90's [1], and numerous publications on their control have appeared ever since [2]-[5].

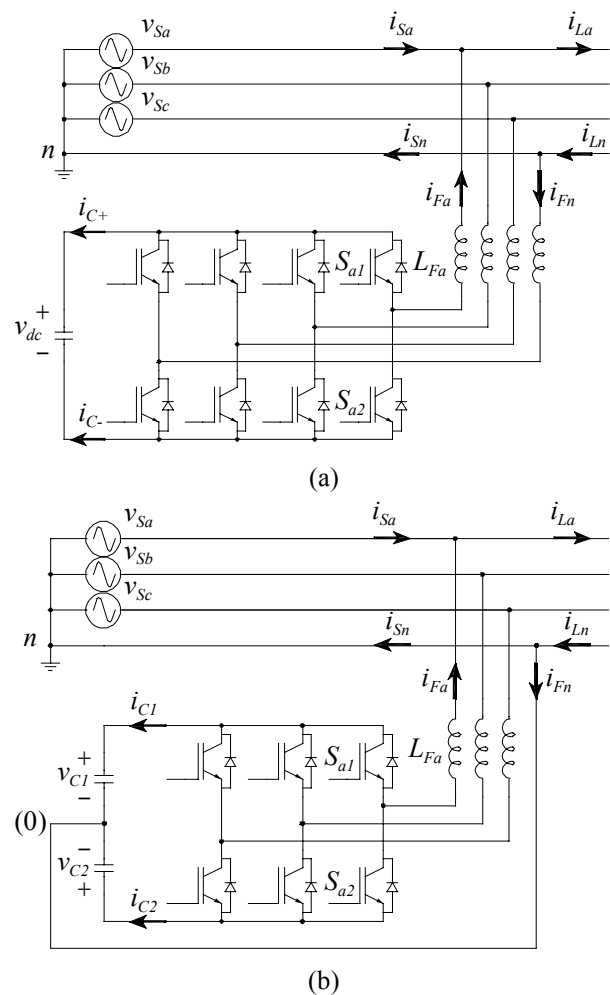


Fig. 1. Active power filter based in:  
(a) FLFB converter. (b) TLSC converter

The FLFB converter shows better controllability thanks to its greater number of semiconductor devices.

However, the interaction between the legs connected to the utility phases and the leg connected to the neutral conductor makes necessary space-vector based current control in order to achieve suitable reference current tracking. The TLSC converter, having a smaller number of switches, permits each of the three legs to be controlled independently, making its current tracking control simpler than the previous topology. However, in this case all the zero-sequence injected current flows through the dc-bus capacitors. This current gives rise to imbalance in the capacitors voltage sharing, forcing to increase the capacitors rating to constantly ensure that capacitor voltages have a sufficiently high absolute value.

Merging topologies shown in Fig. 1, an alternative topology, shown in Fig. 2 and recently presented for active filter applications [6]-[7], can be obtained. This Four-Leg Split-Capacitor (FLSC) topology solves the cited problems of the previous topologies. In this work, the study of FLSC topology will allow to obtain an average model that will hugely accelerate the simulation tasks for this kind of applications. Besides, it will be evidenced that the obtained model also depicts the behaviour of FLFB and TLSC converters, and even contemplates the behaviour of the Three-Legs Full-Bridge (TLFB) converter for three-wire applications.

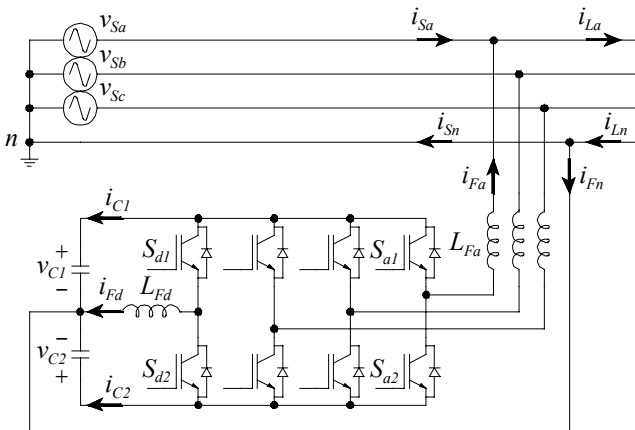


Fig. 2. Active power filter based in FLSC converter

## 2. Phase-leg average model

The switching elements in Fig. 2 can be described by a generic switch  $S$  shown in Fig. 3, whose control function is exposed in (1).

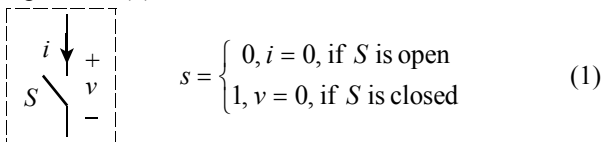


Fig. 3. Generic switch  $S$

In the current-bidirectional switch based converters, a generic switching unit, called switching-leg, can be identified, as shown in Fig. 4 which  $i = \{a, b, c, d\}$ . Each leg is composed of two switching elements, and has a voltage source (or a capacitor) on one side and a current source (or an inductor) on the other. These features make the phase leg a generic switching unit.

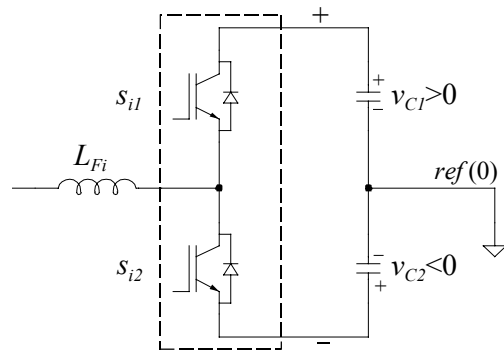


Fig. 4. Generic switching-leg in current-bidirectional converters

The necessary compatibility between switching-leg states is guaranteed if it is accomplished that:

$$s_{i1} + s_{i2} = 1 \quad (2a)$$

$$s_{i1} \cdot s_{i2} = 0 \quad (2b)$$

As a result, the switching-leg can be represented by a single-pole, double-throw switch, as shown in Fig. 5. In this figure, the input and output variables of interest are also defined.

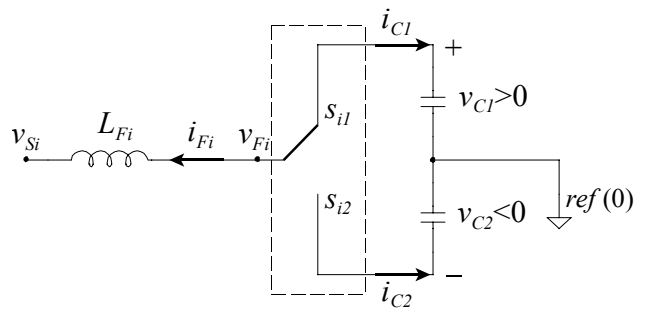


Fig. 5. Switching-leg represented as a single-pole, double-throw switch

Supposing  $C_1=C_2=C$ , a simple analysis of circuit shown in Fig. 5, permits to obtain the expressions (3) and (4), which relate the different variables in each switching interval. In these expressions  $T_{Si}$  is the switching period, and  $d_i \in [0, 1]$  is the duty cycle of the leg.

$$t \in [0, d_i T_{Si}] \left\{ \begin{array}{l} \frac{d}{dt} i_{Fi} = \frac{1}{L_{Fi}} (v_{C1} - v_{Si}) \\ \frac{d}{dt} v_{C1} = -\frac{1}{C} i_{Fi} \\ \frac{d}{dt} v_{C2} = 0 \end{array} \right. \quad (3)$$

$$t \in [d_i T_{Si}, T_{Si}] \left\{ \begin{array}{l} \frac{d}{dt} i_{Fi} = \frac{1}{L_{Fi}} (v_{C2} - v_{Si}) \\ \frac{d}{dt} v_{C1} = 0 \\ \frac{d}{dt} v_{C2} = -\frac{1}{C} i_{Fi} \end{array} \right. \quad (4)$$

From (3) and (4), the generic switching-leg can be represented by means of a state-space average model, in

which the state equation is (5a) and the output equation is (5b). To simplify notation, variables in these equations represent averaged values over a switching period, that is:  $i_{Fi} \equiv \bar{i}_{Fi}$ ,  $v_{Si} \equiv \bar{v}_{Si}$ , etc.

(5a)

$$\begin{bmatrix} \dot{i}_{Fi} \\ \dot{v}_{C1} \\ \dot{v}_{C2} \end{bmatrix} = \begin{bmatrix} 0 & \frac{d_i}{L_{Fi}} & \frac{(1-d_i)}{L_{Fi}} \\ -\frac{d_i}{C} & 0 & 0 \\ -\frac{(1-d_i)}{C} & 0 & 0 \end{bmatrix} \begin{bmatrix} i_{Fi} \\ v_{C1} \\ v_{C2} \end{bmatrix} + \begin{bmatrix} -\frac{1}{L_{Fi}} \\ 0 \\ 0 \end{bmatrix} v_{Si}$$

$$\begin{bmatrix} v_{Fi} \\ i_{C1} \\ i_{C2} \end{bmatrix} = \begin{bmatrix} 0 & d_i & 1-d_i \\ -d_i & 0 & 0 \\ -(1-d_i) & 0 & 0 \end{bmatrix} \begin{bmatrix} i_{Fi} \\ v_{C1} \\ v_{C2} \end{bmatrix} \quad (5b)$$

Now, a new control variable  $c_i \in [-1, 1]$  is defined, and its relationship with  $d_i$  is shown in (6).

$$c_i = -1 + 2d_i \quad (6a)$$

$$d_i = \frac{1+c_i}{2} \quad ; \quad 1-d_i = \frac{1-c_i}{2} \quad (6b)$$

Then, the state-space equations shown in (3) can be expressed as:

$$\begin{bmatrix} \dot{i}_{Fi} \\ \dot{v}_{C1} \\ \dot{v}_{C2} \end{bmatrix} = \begin{bmatrix} \frac{1}{L_{Fi}} & 0 & 0 \\ 0 & \frac{1}{C} & 0 \\ 0 & 0 & \frac{1}{C} \end{bmatrix} \mathbf{A} \begin{bmatrix} i_{Fi} \\ v_{C1} \\ v_{C2} \end{bmatrix} + \begin{bmatrix} -\frac{1}{L_{Fi}} \\ 0 \\ 0 \end{bmatrix} v_{Si} \quad (7a)$$

$$\begin{bmatrix} v_{Fi} \\ i_{C1} \\ i_{C2} \end{bmatrix} = \mathbf{A} \begin{bmatrix} i_{Fi} \\ v_{C1} \\ v_{C2} \end{bmatrix} \quad (7b)$$

where:

$$\mathbf{A} = \frac{1}{2} \begin{bmatrix} 0 & 1+c_i & 1-c_i \\ -(1+c_i) & 0 & 0 \\ -(1-c_i) & 0 & 0 \end{bmatrix} \quad (7c)$$

Based on (7b), the averaged output voltage of the switching leg can be written as:

$$v_{Fi} = \frac{1}{2} [(1+c_i)v_{C1} + (1-c_i)v_{C2}] = \frac{1}{2} (c_i v_{dc} + \Delta v_{dc}) \quad (8)$$

where  $v_{dc} = v_{C1} - v_{C2}$  represents the *dc-bus absolute voltage*, and  $\Delta v_{dc} = v_{C1} + v_{C2}$  represents the *dc-bus differential voltage*. Now, the control variable  $c_i$  can be expressed as a function of the leg voltages, obtaining:

$$c_i = \frac{2v_{Fi} - \Delta v_{dc}}{v_{dc}} \quad (9)$$

Substituting (9) in (7b), and taking into account that the averaged value of leg output voltage is:

$$v_{Fi} = v_{Si} + L_{Fi} \frac{di_{Fi}}{dt}, \quad (10)$$

then the current in capacitors are given by:

$$i_{C1} = \frac{1}{v_{dc}} \left( v_{C2} i_{Fi} - v_{Si} i_{Fi} - L_{Fi} i_{Fi} \frac{di_{Fi}}{dt} \right) \quad (11a)$$

$$i_{C2} = \frac{1}{v_{dc}} \left( -v_{C1} i_{Fi} + v_{Si} i_{Fi} + L_{Fi} i_{Fi} \frac{di_{Fi}}{dt} \right) \quad (11b)$$

From (8) and (11), the average model of the switching-leg controlled by  $c_i$  is shown in Fig. 6. Note that node  $m$  is virtually connected to the reference node.

### 3. Four-wire active filter average model

Once the average model of the switching-leg is justified, the average model of the active filter is readily obtained by connecting four averaged switching-legs and the rest of the circuit components. In Fig. 7, a universal model is shown. This model, besides describing the behaviour of four-leg active filters shown in Figs. 1 and 2, it also contemplates the behaviour of the three-leg four wire converters for three-wire systems (TLFB).

From (7), the four-wire model can be depicted by the state equations shown in (12).

$$\dot{\mathbf{I}}_F = \frac{1}{L_F} \cdot (\mathbf{C} \cdot \mathbf{V}_C - \mathbf{V}_S) \quad ; \quad \dot{\mathbf{V}}_C = -\frac{1}{C} \cdot \mathbf{C}^T \cdot \mathbf{I}_F \quad (12)$$

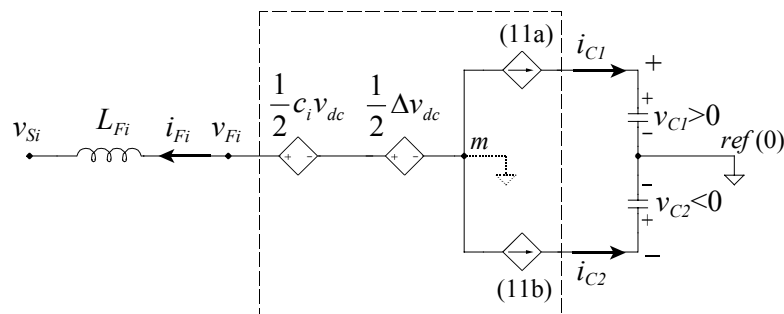


Fig. 6. Average model of the switching leg controlled by  $c_i$

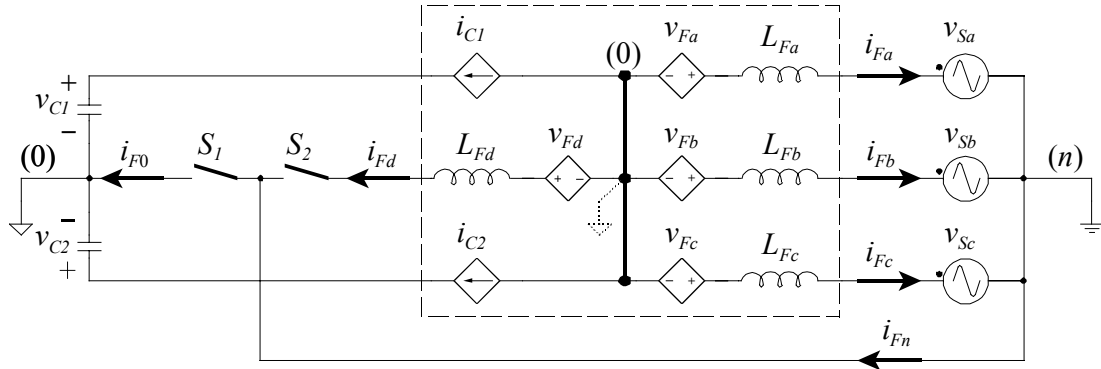


Fig. 7. Universal average model of shunt active power filters

where  $L_{Fi} = L_F \forall i_{i=\{a,b,c,d\}}$ ,  $C_1=C_2=C$ , and

$$\mathbf{I}_F = [i_{Fa} \quad i_{Fb} \quad i_{Fc} \quad i_{Fd}]^T \quad (13a)$$

$$\mathbf{V}_C = [v_{C1} \quad v_{C2}]^T \quad (13b)$$

$$\mathbf{V}_S = [v_{Sa} \quad v_{Sb} \quad v_{Sc} \quad 0]^T \quad (13c)$$

$$C = \frac{1}{2} \begin{bmatrix} (1+c_a) & (1-c_a) \\ (1+c_b) & (1-c_b) \\ (1+c_c) & (1-c_c) \\ (1+c_d) & (1-c_d) \end{bmatrix} \quad (13d)$$

In Fig. 7,  $S_1$  and  $S_2$  represent generic switches like those shown in Fig. 3, and in function of their control variables, the model of this figure describes the behaviour of the converters enumerated in Table I.

TABLE I. – Active filter topologies as a function of  $s_1$  and  $s_2$

$s_1$	$s_2$	Converter	Variables
0	0	TLFB	$v_{0n} \neq 0$ ; $i_{F0} = i_{Fd} = i_{Fn} = 0$
0	1	FLFB	$v_{0n} \neq 0$ ; $i_{F0} = 0$ ; $i_{Fd} = -i_{Fn}$
1	0	TLSC	$v_{0n} = 0$ ; $i_{F0} = i_{Fn}$ ; $i_{Fd} = 0$
1	1	FLSC	$v_{0n} = 0$ ; $i_{F0} = i_{Fd} + i_{Fn}$

For  $s_1=0$ , and taking into consideration an active filter implemented by means of FLFB converter, voltages of model in Fig. 7 can be written as (14), where  $i=\{a,b,c,d\}$ , and  $v_{Sd-n}=0$ .

$$v_{Fi-n} = L_{Fi} \frac{di_{Fi}}{dt} + v_{Si-n} = v_{Fi-0} + v_{0n} \quad (14)$$

Taking into account that in FLFB converter:

$$\sum_{i=a,b,c,d} i_{Fi} = 0 \Big|_{\substack{i_{F0}=0 \\ i_{C1}=-i_{C2}}} \quad \text{and} \quad (15)$$

$$L_F \sum_{i=a,b,c,d} \frac{di_{Fi}}{dt} = 0, \quad (16)$$

then (14) can be expressed as (17).

$$\sum_{i=a,b,c,d} v_{Fi-n} = \sum_{i=a,b,c} v_{Si-n} = \sum_{i=a,b,c,d} v_{Fi-0} + 4v_{0n} \quad (17)$$

Therefore, voltage between the utility neutral point ( $n$ ) and the reference node ( $0$ ) will be:

$$v_{0n} = \frac{1}{4} \left( \sum_{i=a,b,c,d} v_{Si-n} - \sum_{i=a,b,c,d} v_{Fi-0} \right) \quad (18)$$

The expression (18) would also be valid for the three-leg full-bridge converter (TLFB), with the only exception of considering  $v_{Fd-0}=0$  and assigning a value of 1/3 to the multiplier constant.

Expression for current flowing through capacitors in Fig. 7 will be obtained by the sum of terms shown in (11) for the different legs, keeping in mind that  $v_{Sd}=0$ . See (19).

$$i_{C1} = \frac{1}{v_{C1} - v_{C2}} \left[ v_{C2} \sum_{i=a,b,c,d} i_{Fi} - \sum_{i=a,b,c} v_{Si} i_{Fi} \dots \dots - L_F \sum_{i=a,b,c,d} \left( i_{Fi} \frac{di_{Fi}}{dt} \right) \right] \quad (19a)$$

$$i_{C1} = \frac{1}{v_{C1} - v_{C2}} \left[ -v_{C1} \sum_{i=a,b,c,d} i_{Fi} + \sum_{i=a,b,c} v_{Si} i_{Fi} \dots \dots + L_F \sum_{i=a,b,c,d} \left( i_{Fi} \frac{di_{Fi}}{dt} \right) \right] \quad (19b)$$

Or also:

$$i_{C1} = \frac{1}{v_{dc}} \left[ v_{C2} i_{F0} - p_F - L_F \sum_{i=a,b,c,d} \left( i_{Fi} \frac{di_{Fi}}{dt} \right) \right] \quad (20a)$$

$$i_{C1} = \frac{1}{v_{dc}} \left[ -v_{C1} i_{F0} + p_F + L_F \sum_{i=a,b,c,d} \left( i_{Fi} \frac{di_{Fi}}{dt} \right) \right] \quad (20b)$$

where  $i_{F0}$  is the injected current in dc-bus midpoint, and  $p_F$  is the instantaneous active power developed by the filter.

Supposing  $v_{C1}(0) = -v_{C2}(0)$ , dc-bus differential voltage will be given by (21).

$$\Delta v_C = \frac{1}{C} \int_0^t (i_{C1} + i_{C2}) dt \quad (21)$$

And taking into account (20), then:

$$\Delta v_C = \frac{1}{C} \int_0^t \left( \frac{v_{C2} - v_{C1}}{v_{dc}} \cdot i_{F0} \right) dt = -\frac{1}{C} \int_0^t i_{F0} dt \quad (22)$$

Equation (22) evidences, as logic, that *dc-bus differential voltage* lineally depends on injected current in dc-bus midpoint.

Moreover, energy stored in dc-bus will be calculated by means of (23).

$$w_{dc} = \int_0^t (v_{C1} i_{C1} + v_{C2} i_{C2}) dt + w_{dc}(0) \quad (23)$$

And substituting (20), then:

$$w_{dc} = -\int_0^t \left( p_F + L_F \sum_{i=a,b,c,d} i_{Fi} \frac{di_{Fi}}{dt} \right) dt + w_{dc}(0) \quad (24)$$

In this last equation, it can be appreciated how energy stored in dc-bus depends on the instantaneous active power developed by the filter and on the energy stored in the coupling inductances.

#### 4. Injected current control

Based on what exposed in Section 3, utility connection of a leg in a four-wire generic filter is described by circuit shown in the Fig. 8. The source  $v_{0n}$  corresponds to (18) and it represents the voltage that relates the different legs in full-bridge converters. Therefore, this circuit leads to the diagram show in Fig. 9.

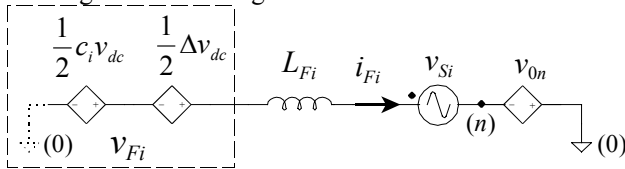


Fig. 8. Utility connection circuit of a leg in a four-wire generic filter

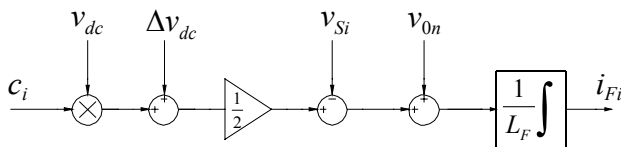


Fig. 9. Utility connection diagram of a leg in a four-wire generic filter

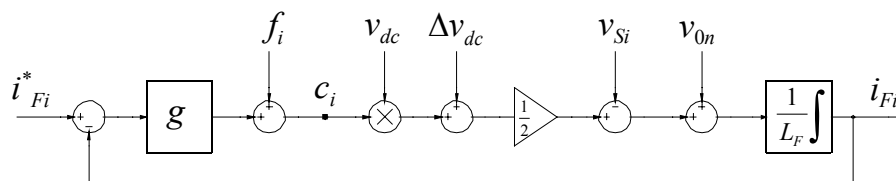


Fig. 10. Current control schema for a leg in four-wire active power filter

From diagram shown in Fig. 9, the evolution of injected current by a leg in four-wire active filter can be expressed by:

$$\frac{di_{Fi}}{dt} = \frac{1}{L_F} \left[ \frac{1}{2} (c_i v_{dc} + \Delta v_{dc}) - v_{Si} + v_{0n} \right] \quad (25)$$

In (25) it can be observed that injected current evolution not only depends on control variable  $c_i$  and dc-bus voltage, but it is also affected by the dc-bus voltage imbalance, the utility voltage, and the behaviour of the rest of legs. Keeping in mind that all these voltages are measurable or evaluable, a schema for current control shown in Fig. 10 is proposed, where a feed-forward signal  $f_i$  has been applied, being:

$$f_i = \frac{1}{v_{dc}} \left[ -\Delta v_{dc} + 2v_{Si} - 2v_{0n} \right] \quad (26)$$

With the control schema shown in the Fig. 11 will be achieved that:

$$\frac{di_{Fi}}{dt} = \frac{1}{L_F} \left\{ \left[ (i_{Fi}^* - i_{Fi}) * g \right] \frac{v_{dc}}{2} \right\} = \frac{1}{2L_F} c_i v_{dc} \quad (27)$$

where the symbol '\*' represents the convolution product of current error signal and the temporal expression of the chosen controller,  $g$ . In (27) injected current control now only depends on the control variable  $c_i$ , and on the actual dc-bus voltage, so decoupling between legs has been achieved, which is a great advantage in full-bridge converters, since now is not necessary to use space-vector based techniques for the injected current control.

#### 5. Conclusions

The average model presented in this work offers valuable contributions in the design and simulation tasks of current compensation systems for four-wire networks, since it is completely generic, being able to simulate the different topologies used in these applications by means of acting on two switches.

The computational cost that presents the proposed model, regarding the commuted model is minimum, obtaining reliable simulations results in infinitely inferior time.

The technique presented for the injected current control is also generic, presenting as main advantage a decoupled control of the different legs, so full-bridge converters can be implemented without using space-vector based current control techniques.

## References

- [1] C.A. Quinn and N. Mohan, "Active Filtering Currents in Three-Phase, Four-Wire Systems with Three-Phase and Single-Phase Non-Linear Loads", in *Proceedings of the 1992 IEEE Applied Power Elect. Conf.*, pp. 829-836.
- [2] M. Aredes, J. Hafner, and K. Heumann, "Three-phase Four-wire Shunt Active Filters Control Strategies", *IEEE Trans. Power Electronics*, vol. 12, no. 2, March 1997, pp. 311-318.
- [3] P. Verdelho, and G.D. Marques, "Four-wire Current-Regulated PWM Voltage Converter", *IEEE Trans. Industrial Electronics*, vol. 45, no. 5, Oct. 1998, pp. 761-770.
- [4] P. Verdelho, "Space Vector Based Current Controller in  $\alpha\beta 0$  Coordinate System for the PWM Voltage Converter Connected to the AC Mains", in *Proceedings of the 1997 IEEE Power Elect. Spec. Conf.*, pp. 1115-1120.
- [5] R. Zhang, V.H. Prasad, D. Boroyevich and F.C. Lee, "Three-Dimensional Space Vector Modulation for Four-Leg Voltage-Source Converters", *IEEE Trans. Power Electronics*, vol. 17, no. 3, May 2002, pp. 314-326.
- [6] M.K. Mishra, A. Joshi and A. Ghosh, "Control Strategies for Capacitor Voltage Equalization in Neutral Clamped Shunt Compensators", in *Proceedings of the 2001 IEEE Power Eng. Society Winter Meeting*, vol. 1, pp. 132-137.
- [7] P. Rodríguez, R. Pindado and J. Bergas, "Alternative Topology for Three-Phase Four-Wire PWM Converters Applied to a Shunt Active Power Filter", in *28<sup>th</sup> Annual IEEE Conf. of the Industrial Electronics Society*, vol. 4, Nov. 2002, pp. 2939-2944.